JCI The Journal of Clinical Investigation

Phase I study of adjuvant immunotherapy with autologous tumor-infiltrating lymphocytes in locally advanced cervical cancer

He Huang, … , Ji-Hong Liu, Jiang Li

J Clin Invest. 2022. https://doi.org/10.1172/JCI157726.

Clinical Medicine In-Press Preview Clinical trials Oncology

BACKGROUND. Adoptive cell therapy (ACT) with tumor-infiltrating lymphocytes (TILs) has achieved remarkable clinical efficacy in metastatic cancers such as melanoma and cervical cancer (CC). Here we explored the safety, feasibility and preliminary tumor response and performed translational investigations of adjuvant immunotherapy using infusion of autogenous (auto)-TILs following concurrent chemoradiotherapy (CCRT) in CC patients with locally advanced disease.

METHODS. Twenty-seven CC patients with stage III to IV disease were recruited in this single-center, phase I study. TILs were isolated from lesions in the uterine cervix and generated under good manufacturing practices (GMP) conditions and then infused after CCRT plus intramuscular interleukin (IL)-2 injections.

RESTULTS. From 27 patients, TILs were successfully expanded from 20 patients, with a feasibility of 74.1%. Twelve patients received TILs following CCRT. Adverse events (AEs) were primarily attributable to CCRT. Only 1 (8.3%) patient experienced severe toxicity with a grade 3 hypersensitivity reaction after TIL infusion. No autoimmune AEs, such as pneumonitis, hepatitis, or myocarditis, occurred, and there was no treatment-related mortality. Nine of 12 patients (75.0%) attained complete response, with a disease control duration of 9 to 22 months. Translational investigation showed that the transcriptomic characteristics of […]

Phase I study of adjuvant immunotherapy with autologous tumor-infiltrating lymphocytes in locally advanced cervical cancer

He Huang[1,3], Cai-ping Nie[1,2], Xiu-feng Liu[1,2], Bin Song[6,7], Jian-hui Yue[6,8], Jing-xiao Xu[1,2], Jia He[1,2], Kui Li[1,2], Yan-lin Feng[1,3], Ting Wan[1,3], Min Zheng[1,3], Yan-Na Zhang[1,3], Wei-Jun Ye[1,4], Jun-Dong Li[1,3], Yan-Fang Li[1,3], Jun-yun Li[1,4], Xin-Ping Cao[1,4], Zhi-min Liu[1,3], Xiao-shi Zhang[1,2], Qing Liu[1,6], Xi Zhang[6], Ji-Hong Liu[1,3], Jiang Li[1,2]

[1]State Key Laboratory of Oncology in South China; Collaborative Innovation Center for Cancer Medicine; [2]Department of Biotherapy, [3]Department of Gynecological Oncology, Sun Yat-sen University Cancer Center; [4]Department of Radiation Oncology, [5]Department of Cancer Prevention Research, Sun Yat-sen University Cancer Center; [6]BGI-Shenzhen, Shenzhen, China; [7]College of Life Sciences, University of Chinese Academy of Sciences, Beijing, China; [8]Section of Cell Biology and Physiology, Department of Biology, University of Copenhagen, Copenhagen, Denmark.

Running title: Phase I study of concurrent chemoradiotherapy and TIL immunotherapy in cervical cancer

Authorship note: HH, CPN, XFL, BS and JHY are co-first authors and contributed equally to this work. JL, JHL and XZ are co-senior authors and contributed equally to this work.

Email address: lijiang@sysucc.org.cn

23 Department of Biotherapy, Sun Yat-sen University Cancer Center

24 Address: 651 Dongfeng East Road, Guangzhou, 510060, China

Abstract

BACKGROUND. Adoptive cell therapy (ACT) with tumor-infiltrating lymphocytes (TILs) has achieved remarkable clinical efficacy in metastatic cancers such as melanoma and cervical cancer (CC). Here we explored the safety, feasibility and preliminary tumor response and performed translational investigations of adjuvant immunotherapy using infusion of autogenous (auto)-TILs following concurrent chemoradiotherapy (CCRT) in CC patients with locally advanced disease.

METHODS. Twenty-seven CC patients with stage III to IV disease were recruited in this single-center, phase I study. TILs were isolated from lesions in the uterine cervix and generated under good manufacturing practices (GMP) conditions and then infused after CCRT plus intramuscular interleukin (IL)-2 injections.

RESTULTS. From 27 patients, TILs were successfully expanded from 20 patients, with a feasibility of 74.1%. Twelve patients received TILs following CCRT. Adverse events (AEs) were primarily attributable to CCRT. Only 1 (8.3%) patient experienced severe toxicity with a grade 3 hypersensitivity reaction after TIL infusion. No autoimmune AEs, such as pneumonitis, hepatitis, or myocarditis, occurred, and there was no treatment-related mortality. Nine of 12 patients (75.0%) attained complete response, with a disease control duration of 9 to 22 months. Translational investigation showed that the transcriptomic characteristics of the infused TIL products and some immune biomarkers in the tumor microenvironment and serum of CC patients at baseline were correlated with the clinical response.

CONCULSION. TIL-based ACT following CCRT was safe in an academic center

setting, with potential effective responses in locally advanced CC patients. ‘Hot’ inflammatory immune environments are beneficial to the clinical efficacy of TIL-based ACT as adjuvant therapy.

TRIAL REGISTRATION. ClinicalTrials.gov NCT04443296.

FUNDING. National Key R&D Program; Sci-Tech Key Program of the Guangzhou City Science Foundation; the Guangdong Province Sci-Tech International Key Program; the National Natural Science Foundation of China.

Introduction

Cervical cancer (CC) is the fourth most common cancer and represents one of the leading causes of cancer-related mortality in women worldwide, with approximately 570,000 new cases and 311,000 deaths annually (1). Concurrent chemoradiotherapy (CCRT) is the standard treatment for patients with locally advanced CC (2). However, the improvement in long-term outcomes seems to be more pronounced for patients with stage IB-IIB cancers than for those with stage III and IVA cancers (3). The prognosis of patients with advanced stage disease remains poor, with 5-year survival rates for stage III and IVA of 39.3% and 24%, respectively (4), which highlights the need for novel therapeutic methods combined with CCRT as the primary treatment.

Adoptive cell therapy (ACT) using autologous tumor-infiltrating lymphocytes (auto-TILs) has been under development in melanoma since the 1980s and can induce complete tumor responses in some patients (5-8). Recently, TIL-based ACT has been used in HPV-positive oropharyngeal, anal and cervical cancer patients and has shown some clinical activity (9-11), which is worth further investigation. Recently, accumulating evidence has identified that TIL-based ACT treatment is beneficial for some metastatic cancers, including some patients with checkpoint inhibition immunotherapy resistance (5, 12-14). However, some researchers point out that TIL-based ACT might be used prior to other immunotherapies in eligible patients (15, 16). We have established the primary treatment pattern of TIL-based ACT combined with CCRT in EBV-positive nasopharyngeal carcinoma patients with advanced

disease stages, and the objective clinical response and EBV-specific reactivity of T cells were observed in some patients (17).

In this clinical trial, we first established an ex vivo 'young' TIL expansion method under standard good manufacturing practices (GMP) conditions from transvaginally biopsied small tumor fragments. We sought to investigate the safety of this TIL-based ACT following CCRT in CC patients with locally advanced disease; feasibility and clinical activity were also preliminarily evaluated. Correlates between immune parameters and clinical response were evaluated to screen for potential biomarkers for the clinical benefit of TIL-based ACT as adjuvant therapy.

Results

Patients and feasibility

A total of 27 patients with CC were enrolled between December 2019 and 17 December 2020. The average age was 56 years (range 42-70). Of 27 patients, 24 were diagnosed with squamous cell carcinoma (SCC) and 3 were diagnosed with adenocarcinoma (AC). The FIGO stage was III-IV (25 for stage III and 2 for stage IV). Detailed patient information is shown in Supplemental Table 1. Biopsies of carcinoma in the cervix uteri (n =26) and metastatic cancer in the lung (n =1) were collected. Purified lymphocytes were successfully obtained from 20 samples of 27 recruited patients, and expanded TILs were established ex vivo under GMP conditions, with a feasibility of 74.1% (20/27). The remaining 7 samples failed to establish ex vivo-expanded TILs due to contamination (5/27, 18.5%) and an insufficient

lymphocyte number for expansion (2/27, 7.4%). Among the 20 patients with successfully expanded TILs, 13 of them received auto-TIL infusion plus intramuscular interleukin (IL)-2 injection following CCRT. In total, 14 patients received CCRT treatment only (radical radiotherapy for CC and weekly cisplatin with external radiotherapy), including 2 patients who refused infusion, 5 patients who were hindered by the influence of COVID-19, and the 7 patients who failed to establish expanded TILs, as shown in Figure 1.

Of the 13 patients who received auto-TIL infusion plus intramuscular IL-2 injection, 11 tumors were classified as SCC, and 2 were classified as AC (Table 1). Among them, 12 patients received CCRT treatment and were included in the safety and efficacy analysis. Patient No. 1 was excluded because lung metastasis was found and diagnosed as stage IVB; thus, the patient did not receive CCRT but received systemic chemotherapy firstly with paclitaxel and cisplatin instead, followed by auto-TIL infusion plus intramuscular IL-2 injection.

Safety and adverse events (AEs)

AEs were mostly attributable to CCRT. The most common severe AEs were hematological and gastrointestinal toxicities during chemoradiotherapy in patients who received CCRT followed by TIL infusion. No treatment-related mortalities occurred. The toxicity profile was consistent with that of CCRT only (Table 2). Grade 1 or 2 toxicities were common and included nausea, vomiting, diarrhea and constipation. Fatigue was observed in 33.3% patients. Grade 3 or 4 toxicities were hematological during chemoradiotherapy. Anemia was the most common AE. No

unexpected toxicity was observed, and all adverse reactions were manageable following standard guidelines.

Three AEs, including 1 (1/12, 8.3%) severe toxicity, were related to TIL infusion. Patient No. 19 experienced a grade 3 hypersensitivity reaction 30 min after auto-TIL infusion with a decrease in blood pressure, dizziness and mild dyspnea. The symptoms resolved after intravenous epinephrine and dexamethasone. According to pre-specified criteria for the safety end point, this event was defined as severe toxicity. This patient achieved complete regression (CR) 4 months after treatment. The other grade 1 or 2 AEs included 1 allergy with itchy skin and mild rash and another with fatigue. No autoimmune AEs, such as pneumonitis, colitis, hepatitis, nephritis, or myocarditis, appeared, and no treatment-related mortalities occurred. Seven patients (58.3%) experienced low fever after IL-2 injection; the symptoms resolved after IL-2 injection without any antipyretic treatment. The AEs of all patients with or without auto-TIL infusion plus intramuscular IL-2 injection following CCRT are summarized in Table 2.

Clinical activity

Until the last follow-up on March 1st, 2022, 9 of 12 patients with TIL infusion (75.0%) attained CR of one or more tumors, with a disease control duration of 9 to 22 months (Table 1). Five patients (No. 2, 4, 22, 23 and 26) achieved a CR 3 months after CCRT and TIL infusion; however, Patient No. 22 experienced a PD after 14 months of CR (Figure 2, A-B). The other 5 patients (Patient No.10, 11, 18, 19, and 25) experienced a partial response after 3 month of treatment and then attained a CR in

the following 2 to 5 months, such as Patient No. 19 and Patient No. 11 (Figure 2, C-D). No deaths occurred among these 12 patients, and the mean PFS and OS times were 23 and 25 months, respectively.

Among the 14 patients who received CCRT only, one patient refused treatment and was lost to follow-up. Two patients died because of their disease 16 and 11 months after CCRT treatment. The death rate was 15.4% (2/13). Nine patients (9/13, 69.2%) achieved CR, and 2 (2/13, 15.4%) achieved PR (Table 1).

Correlates between clinical response and immune parameters

Characteristics of infused TIL products

We analyzed the biological characteristics of the infused TIL products by flow cytometry and IFNγ ELISPOT array (n = 13) and scRNA-seq (n = 8, Figure 3A). First, we observed that the reactivity of T cells against HPV E6 and E7 antigens was enriched in TIL products relative to circuiting T cells, and most TILs were comprised of $CD3^+CD4^+$, $CD3^+CD8^+$ and $CD3^+CD56^+$ cells (Supplemental Figure 1, A-D). No associations were found between the frequency of E6- or E7-specific T cells and the composition of the TIL subset and patient clinical efficacy in this study (Figure 3, B-C). We further found that the majority of infused TILs were $PD\text{-}1^+Tim3^-CXCR5^+$ central memory cells, and an increased CD137 expression level was found in the rapidly expanded infused TIL products (Supplemental Figure 1, C-D). Furthermore, scRNA-seq analysis showed that cells from 8 TIL productions were interspersed across multiple clusters and defined as $CD8^+$ and $CD4^+$ cell clusters based on filtered and normalized transcript counts. The cell clusters from the scRNA-seq array were

verified by FACS gating strategy analysis (Figure 3D and Supplemental Figure 1, E-F). Genes related to proliferation and cytotoxicity as well as T cell immune checkpoints were visualized on the CD3, CD8 and CD4 cell subsets (Figure 3E). Differentially expressed gene (DEG) analysis showed that the genes related to cell differentiation and activation, including *CTSW*, *NKG7*, *GNLY*, *MKI67*, and *STAT1*, had a high level in responders vs. nonresponders (n = 4 and 4, respectively, Figure 3F). The activation and proliferation signaling pathways as well as the levels of cytotoxic, proliferation and mutation-associated neoantigen (MANA)-specific T cell signatures were upregulated in responders' TIL infusion products, but the dysfunctional cell signature was downregulated (Figure 3, G and H). We further determined the anti-tumor reactivity of the infused TIL products by detecting INFγ release and cytotoxicity against SiHa (HPV+, partly MHC-matched) cells in vitro (Figure 4, A-B), as well as SiHa-tumor growth inhibition in nude mice (Figure 4, C-D). Importantly, no observable toxicity was found in SiHa tumor-bearing nude mice infused with human TILs isolated from CC patients (partly MHC matched), and infiltration of the infused TILs into tumor tissues was observed (Figure 4, E-F).

Peripheral and tumor immune parameters

In the exploration analysis, we further investigated feasible predictors for the clinical benefit of auto-TIL treatment based on the tumor and peripheral immune parameters of patients at baseline and after CCRT or TIL-based ACT treatment. We found that a combined immune score calculated based on the levels of immune inhibitory factors (PD-L1, TOX and Foxp3) and immune stimulatory factors (CD4,

CD8, CD20, CD56 and TLS), as shown in the Method section, displayed a higher level in nonresponders at baseline ($P < 0.05$), and the CCRT treatment relieved immune suppression factors such as TOX ($P < 0.05$) and induced more infiltrated lymphocytes in tumor tissues (Figure 5, A-C). We did not observe an association between the alteration of peripheral HPV E6 or E7 antigen-specific T cells or immune cell subsets, including $CD3^+$T cells, $CD3^+CD4^+$T cells, $CD3^+CD8^+$T cells, $CD3^-CD16^+$NK cells, $CD4^+$ $CD25^+Foxp3^+$ Tregs, $PD1^+CXCR5^-Tim\text{-}3^-$cells and $PD1^+CXCR5^+Tim\text{-}3^+$cells, and clinical efficacy in this trial (Supplemental Figure 2, A-B). However, the peripheral lymphocyte count was significantly decreased after CCRT treatment compared with baseline ($P < 0.05$, Supplemental Figure 2C). Moreover, responders ($n = 9$) displayed a higher baseline serum level of inflammatory cytokines and chemokines, including TNF-α, IL-12, MCP-1 and fractalkine (CX3CL1), than nonresponders ($n = 3$, $P < 0.05$, Figure 5D). Interestingly, CCRT treatment increased the serum cytokine level of IP-10 but decreased the TNF-α level ($P < 0.05$, Figure 5E). Overall, 'hot' microenvironments with lower levels of inhibitory factors (PD-L1, TOX and Foxp3) and higher levels of infiltrated lymphocytes, including T cells, NK and B cells, as well as mature TLSs, were observed in responders such as Patient Nos. 19 and 11 with CR (Figure 2, E-F). Accordingly, 'cold' microenvironments with higher levels of inhibitory factors and lower levels of infiltrated lymphocytes as well as a low number of mature TLSs were observed in nonresponders such as Patient Nos. 13 and 17 with PD (Supplemental Figure 3).

Discussion

In this trial, we proposed a primary treatment pattern of TIL-based ACT following CCRT in CC patients with advanced-stage disease (FIGO stage IIIA to IVA). For these patients, CCRT with cisplatin remains the standard treatment; however, the survival outcome is unsatisfactory (approximate 3-year overall survival rate of only 32%-45% for stage IVA) (3, 18-22). Thus, it is essential to search for novel therapeutic methods combined with CCRT in primary treatment that would improve the prognosis. Immunotherapies, including immune checkpoint inhibitors or adoptive immune cells, have shown efficacy in the treatment of CC and may provide a longer tumor control period and better survival (23, 24). We successfully established a protocol for a GMP therapy-level TIL expansion approach in vitro from small biopsy samples taken transvaginally from patients and aimed to determine the safety and feasibility of TIL-based ACT following CCRT as adjuvant treatment.

Most clinical trials for TIL-based ACT treatment have been successfully launched in metastatic cancers such as HPV-positive CC, lung cancer and melanoma, and tumor regression has been observed in some cancers; the objective response rate (ORR) ranges from 28% to 50% and changes in cancers of different origins (5-7, 13, 25, 26). However, recently, some researchers have pointed out that the usage of TIL-based ACT prior to other immunotherapeutic strategies in eligible patients may provide a benefit in terms of the clinical response (15, 27); a randomized trial of auto-TIL-based

ACT as adjuvant immunotherapy was reported in stage III melanoma without distant metastasis in 2002, and the researchers updated the follow-up period in 2007 and 2014. This study revealed that after adjusting for the tumor metastatic lymphoid node number, the patients who received auto-TIL-based ACT treatment exhibited a longer relapse-free survival (RFS) and overall survival (OS) compared with the patients who received IL-2 injection only (16, 28, 29). For locally advanced CC (FIGO stage I, stage II with tumor size larger than 4 cm, or stage IIB to IVA) treated with CCRT, the CR rate was reported to range from 62.5% to 81.3% (30, 31). In this study, TIL infusion following CCRT also induced a potent response, with a CR rate of 75% in patients with stage IIIA to IVA disease (disease control time, 9-22 months until the last follow-up) and median PFS and OS times of 23 and 25 months, respectively. The relatively longer disease control period may indicate the potential long-term benefit of auto-TIL infusion. Nevertheless, this clinical achievement should be confirmed in a large sample, phase II study containing a control group with prognostic observations. The toxicities that occurred during TIL therapy were mostly due to lymphodepleting preparative regimens and subsequent IL-2 after TIL infusion. The toxicities related to TIL infusion were less common and may include dyspnea, chills and fever (32, 33). In our study, toxicities were predominantly caused by CCRT, resulting in pancytopenia, gastrointestinal toxicity and fatigue, which were consistent with the toxicity profiles in patients treated by CCRT alone (34). One patient experienced a grade 3 allergic reaction related to TILs shortly after the infusion. The symptoms resolved after intravenous epinephrine and dexamethasone administration. Autoimmune toxicities

were much less common, including vitiligo, hearing loss or uveitis. Uveitis usually responds well to local corticoid treatment (35). Overall, the observed toxicities were manageable for the most part. No specific safety signal of concern was identified for the cells themselves.

It has been mentioned that the roles of radiotherapy and chemotherapy in immune regulation are still controversial. It has been reported that radiotherapy mediates its antitumor effects at least in part by synergizing with the host immune system (36). Some studies have reported that radiotherapy can enhance TAA presentation by DCs to immune cells and enhance the recruitment of antitumor T lymphocytes, such as DCs and $CD8^+$ T cells, in the tumor site by upregulating adhesion molecules (37). On the other hand, radiotherapy can directly inactivate immune cells and lead to the recruitment of myeloid-derived suppressor cells (MDSCs) and Treg cells in the tumor microenvironment, promoting immune tolerance toward tumor cells (38, 39). Thus, it is a reasonable modality with CCRT followed by immunotherapy, such as ACT infusion. In addition, our previous phase I study of CCRT combined with TIL in nasopharyngeal carcinoma showed that CCRT could induce lymphodepletion. In this study, CCRT was also set as a lymphodepletion treatment prior to TIL infusion in consideration of the rationality of the overall treatment scheme and the toxicity of the lymphodepletion regimen. A significant decrease in the lymphocyte count was observed after CCRT (Supplemental Figure 2C). Therefore, we did not implement lymphodepletion with cyclophosphamide and fludarabine, as described in other clinical trials for TIL-based ACT treatment (40).

In addition to the safety and clinical response, we further explored the feasibility of establishing a TIL-based ACT strategy in advanced CC patients. The process of isolating and manufacturing TILs is labor intensive and is only successful in a subset of patients (20-40%); the process is usually restricted by the tumor excision location, size and origin (41-44). However, we could isolate pure lymphocytes from most transvaginal biopsy samples, which were usually of a small size (less than 0.5 cm in diameter), and only 2 of 27 samples failed to establish expanded TILs due to insufficient cell number. It is worth noting that the contamination caused by the open biopsy site (18.5%, 5 of 27) was a major difficulty in establishing successful TILs in this trial. These data suggest that the abundance of TIL in CC tissues allows for a therapeutic level of expanded TIL ($> 10^9$) to be obtained from small biopsy samples, but contamination should be prevented in tumor tissue procured by transvaginal biopsy. For infused TIL product assessment, infused TIL products contained higher levels of HPV E6 and E7 antigen-specific T cells, but we did not observe the correlation of frequencies of HPV E6 and E7 antigen-specific T cells in TILs or peripheral blood and clinical response like another clinical trial of TIL treatment in HPV-positive cancers (9-11). This result may be caused by the small number of patients (several HPV-negative patients were included, Supplemental Table 1) and missing some blood sample collections after TIL infusion due to the influence of COVID-19. However, we demonstrated the function of HPV E6/E7 peptide-specific T cells against SiHa (HPV+) cells in vitro and in vivo (Supplemental Figure 4), and identified that HPV E6/E7 is a potential target against CC. We observed distinct

transcriptomic characteristics of the infused TIL products from responders and nonresponders by scRNA-seq arrays, and the high level of gene clusters related to cytotoxicity, activation and MANA-specific T cell signatures in infused TILs correlated with clinical response. In addition, we further identified the function of infused TIL products by immune responses against SiHa (HPV+) cells in vitro and in vivo. These data suggest that TILs from CC patients was comprised of tumor or associated antigen (neo-antigen)-specific T cells and HPV-antigen specific T cells, both of which may contribute to tumor suppression in TIL-based ACT. Accordingly, immunotherapy based on checkpoint inhibition using PD-1 antibody therapy has archived outstanding clinical outcomes in patients with persistent, recurrent, or metastatic CC who were also receiving chemotherapy (23, 45). These reported results indicate that CC is a highly immunogenic tumor. Thus, TIL-based ACT combined with CCRT may be a beneficial therapeutic strategy for advanced CC patients as an adjuvant therapy to primary treatment.

We further explored the correlations between the clinical response and baseline immune-related biomarkers in this clinical trial. It has been reported that the levels of patient serum cytokines, tumor mutation burden and immune checkpoints as well as the infiltrated immune cell composition may affect and predict the clinical achievement of TIL-based ACT treatment (46-51). Here, we observed that low levels of immune inhibitory factors, such as TOX and Foxp3, and high infiltrated lymphocyte numbers in tumor tissues, as well as high baseline levels of inflammatory cytokines, may predict a clinical benefit for auto-TIL treatment. However, this finding

needs to be confirmed in a large sample with more stringent statistical analysis in the near future. In summary, we found that TIL infusion after CCRT for locally advanced CC was feasible in an academic center setting and had effective responses with tolerable adverse effects, which suggests that further investigation of this setting of therapy in wider populations with CC is worthwhile.

Methods

Study design. The trial was a single-center, phase I study (ClinicalTrials.gov NCT04443296) that aimed to investigate the safety of cisplatin CCRT plus TIL in treating patients with International Federation of Gynecology and Obstetrics (FIGO) stage IIIA to IVA cervical carcinoma. The study was conducted in compliance with the Declaration of Helsinki and Good Clinical Practice guidelines. The protocol was approved by the Ethics Committee of Sun Yat-sen University Cancer Center. All patients provided written informed consent before enrollment.

Patients were treated with external-beam radiotherapy (EBRT) to a dose of 45 Gy for the primary tumor and regional lymphatics at risk. The primary cervical tumor was then boosted using brachytherapy, with an additional 30 to 40 Gy for a total dose of ≥ 85 Gy. During EBRT, cisplatin was given weekly at 30 to 40 mg/m^2 for a maximum of 6 doses. Ex vivo-expanded auto-TILs (>1x10^9 cells in a single dose) were infused 3 days after the completion of CCRT and brachytherapy. After cell infusion, interleukin-2 (IL-2) was administered as an IM bolus at 400,000 IU/dose every 24 hours to 7 doses (Figure 1).

Patients. Patients from 18 to 70 years of age were eligible if they had squamous cell, adenocarcinoma, or adenosquamous carcinoma of the uterine cervix, FIGO stage IIIA to IVA disease. All patients planned to receive prior platinum-based chemoradiotherapy. An Eastern Cooperative Oncology Group performance status of 0 or 1 was required. The target lesion was defined as at least 1 detectable lesion by imaging.

Assessments. The primary objective of the study was to evaluate the safety of CCRT plus auto-TIL in treating patients with FIGO stage IIIA to IVA cervical carcinoma. AEs were recorded from the beginning of CCRT to 30 days following TIL infusion and graded according to the Common Terminology Criteria for Adverse Events (CTCAE), version 5.0. We aimed to evaluate 12 patients for toxicity in this study. Every 3 consecutive patients were treated as a cohort and evaluated for toxicity. If 1 or fewer severe toxicity events related to TIL infusion were observed in the first 3 patients, then 3 more patients were enrolled into the next cohort until 12 patients were included. If ≥2 patients within a cohort experienced severe toxicity events, then that the study would be stopped. Severe toxicity was defined as grade 3 or higher non-autoimmune toxicity suspected to be related to TIL infusion (not related to CC or another pre-existing condition in CCRT), or an autoimmune event that did not resolve with intervention (steroids) to grade 1 or lower within 21 days.

Secondary objectives included feasibility, primarily tumor response and its association with immunologic parameters, PFS and OS. PFS and OS were defined as the time from treatment initiation until progression or death from any cause, respectively, or

the date of data cutoff. Feasibility was defined as the rate of successful TIL generation from tumor biopsy specimens. Tumor response was evaluated according to the RECIST v1.1 guidelines. Objective response was defined as complete regression and partial response. Physical and imaging examinations (MRI/PET-CT/CT) were applied to determine the outcome at 1 month and every 3 months after the treatments.

Generation of TILs. Fresh tumor biopsy specimens were obtained from trans-vaginal biopsy of the lesion and processed for the ex vivo-expansion of 'young' TILs. In brief, fresh tumor samples were collected in Roswell Park Memorial Institute (RPMI) 1640 medium (Gibco) with antibiotics, minced, enzymatically dissociated into single-cell suspensions with collagenase type IV (0.1 mg/mL, Sigma–Aldrich) and then plated into 24-well cell culture plates in X vivo (Lonza) culture medium containing recombinant human IL-2 (1000 IU/mL) for 1 to 2 weeks to obtain purified T cells. Once a sufficient number of T cells (>10 $*10^6$) was generated, the cells were cryopreserved for further expansion. Clinical infusion products were generated by a rapid expansion protocol (REP) for 'young' TILs: Cryopreserved TILs were thawed and further expanded to numbers appropriate for treatment using a human anti-CD3 antibody (clone OKT-3, 30 ng/mL, R&D Systems), 3500 IU/mL human IL-2 (Sihuan Pharmaceutical) and irradiated feeder cells for 14 days under conditions in accordance with current GMP conditions in the Biotherapy Center at Sun Yat-sen University Cancer Center.

Single-cell gene expression sequencing (scRNA-seq) for infused TIL products. All steps from single-cell encapsulation to library preparation were performed at

BGI-Shenzhen, following the manufacturer's instructions. Single-cell capture, cDNA synthesis and preamplification were performed using a DNBelab C4-V1 system (52). Libraries were sequenced on the MGISEQ2000 or DNBSEQ-T1&T5 platform. Raw single-cell RNA-seq data were processed using the DNBelab C Series scRNA-analysis-software (https://github.com/MGI-tech-bioinformatics/DNBelab_C_Series_scRNA-analysis-software), including the gene expression data mapped to the human genome reference sequence (GRCh38). A number of steps were performed to filter out poor-quality data. First, cells with < 200 expressed genes or > 15% of detected genes linked to mitochondrial genes were removed. Second, genes detected in fewer than three cells and cells with more than 7,000 detected genes were filtered out. Third, the R package DoubletFinder (53) was applied to remove doublets, with an expected doublet rate of 0.04. For downstream analyses, the R package Seurat (4.0.0) (54) was applied to normalize the raw count matrix to identify highly variable genes, scale genes, and integrate samples. In addition, the first 20 PCs and 2,000 highly variable genes were used for unsupervised clustering analysis. The umap method performed by the RunUMAP function was used for dimensionality reduction and two-dimensional visualization of the single-cell clusters. Clusters were labeled based on the canonical marker gene expression of the major cell type (CD8 and CD4). Differential expression analysis was performed using the FindMarkers function. Volcano plots were generated using the R package ggplot2 (55) for DEGs. Enrichment analysis to determine the signaling pathways in which the DEGs are involved was then carried

out using gene set enrichment analysis (GSEA) with the R package clusterProfiler (56). Gene set scores of interest were calculated for each cell using the AddModuleScore function (57-59). The raw and processed single-cell sequencing data have been submitted to the Gene Expression Omnibus (GEO) database with the accession number GSE190075.

Flow cytometry. The lymphocyte subsets and immune characteristics of infusion TIL products and the peripheral immune cells from CC patients were detected by fluorescence-activating cell sorter (FACS) staining and detection. Cells were washed twice using phosphate-buffered saline (PBS), labeled with fixable viability dye (eBioscience/Thermo Fisher Scientific) and stained for biomarkers of interest using fluorochrome-conjugated antibodies (anti-human CD3, CD4, CD8, CD56, CD16, CD25, PD-1, TIM3, CXCR5, Foxp3, IFNγ and HLA-A*02:01-E618–26 pentamers) according to the manufacturer's instructions. Detailed antibody information is shown in Supplemental Table 2. Intracellular Foxp3 and IFNγ staining was performed with a fixation/permeabilization solution kit (BD Biosciences) following the instructions of the manufacturer. In brief, cells were stimulated with 10 ng/mL PMA (Sigma–Aldrich), 1 μg/mL ionomycin (Beyotime Biotechnology) and Golgi Stop (BD Biosciences) in complete RPMI 1640 medium (Gibco) for 4-6 hours, permeabilized and fixed for 1 hour, followed by Foxp3 or IFNγ antibody staining. For intracellular staining of Foxp3, a fixation/permeabilization solution kit (BD Biosciences) was used following the instructions of the manufacturer. For intracellular cytokine IFN-γ staining, TILs were cultured for 4-6 hours with 10 ng/mL PMA (Sigma–Aldrich) and

1 μg/mL ionomycin (Beyotime Biotechnology) and Golgi Stop (BD Biosciences) in RPMI 1640 medium. Then, the eBioscience™ Invitrogen™ Intracellular Fixation & Permeabilization Buffer Set (Thermo Fisher Scientific) was used following the instructions of the manufacturer. The frequency of HPV E6-specific reactivity T cells in infusion TIL products and peripheral blood was determined by bound HLA-A*02:01-E618–26 pentamers (peptide sequence: KLPQLCTEL; ProImmune), and at least 10^5 cells were captured by a FACS instrument for pentamer detection. Data were acquired with a Beckman Coulter flow cytometer and analyzed with FlowJo software (Becton and Dickinson). Analyses were gated on live, singlet, lymphocytes. Detailed information on the antibodies and reagents is shown in Supplemental Table 2.

T cell functional assays. The frequency of HPV E6- and E7-specific reactive T cells in the peripheral blood of patients at baseline, before and after TIL infusion and in the infused TIL products was measured by a human IFN-γ precoated ELISpot PRO Kit (Da Ke Wei) according to the manufacturer's instructions. T cells were incubated in this plate at $1*10^5$ cells per well and stimulated with 50 ng/mL of the E6 and E7 proteins (Miltenyi Biotec) or autologous PHA-stimulated blast cells as a control for 20 hours at 37℃. ELISPOTs were developed using AEC plus and counted automatically using ImmunoSpot 5.0.3 analysis software. SFC indicates the number of IFN-γ-producing cells per $1x10^5$ cells after HPV E6/E7 stimulation.

Generation of HPV E6/E7-specific T cells. We generated HPV-E6/E7 peptide-specific T cells in vitro using the following protocol. In brief, peripheral blood mononuclear

cells (PBMCs) isolated from healthy donors and stimulated with 1 μg/mL of the E6 and E7 peptides (Miltenyi Biotec) in X-VIVO medium (Lonza) with 1500 IU/mL IL-2 (Sihuan Pharmaceutical) in an OKT3 precoated 24-well plate for 7 days, restimulated with 1 μg/mL of E6 and E7 peptides and cultured for another 7 days. On day 14, HPV E6/E7 peptide-specific T cells were harvested and analyzed for flow cytometry, LDH cytotoxicity and animal experiments.

Lactate dehydrogenase (LDH) assays. The cytotoxicity analysis of infused TIL products or HPV E6/E7-specific T cells was measured using an LDH assay. The infused TIL products from HLA-matched patients were cocultured with SiHa or 293T cells for 6 hours, and the cell supernatants were collected. LDH activity was measured using an LDH detection kit (Sigma–Aldrich) following the manufacturer's instructions. The data were assessed by optical absorbance on a microplate reader at 490 nm. Cytotoxicity was calculated by the following formula: Cytotoxicity % = (Test Sample - Negative Control) / (Lysate Control - Negative Control) × 100%.

Xenograft mouse model. All animal experiments were performed in accordance with protocols approved by the Institutional Animal Care and Use Committee of SYSU, Guangzhou, China (L102012018060P). The in vivo experiments were performed using 4-week-old female nude athymic mice (BALB/c-nu/nu, Vital River). In brief, after mycoplasma detection by PCR analysis, $5x10^6$ SiHa cells (mycoplasma negative) were resuspended in 100 μL of PBS and injected subcutaneously into the axilla of the right upper limb. After approximately 1 week of transplantation, HLA-matched TILs from cervical cancer patients or HPV E6/E7-specific T cells ($2.5x10^5$, $2.5x10^6$, and

$2.5x10^7$ cells) were injected intravenously into the tail vein for treatment. A xenograft + PBS group was included as a control. Tumor growth was monitored every 3 days, and the tumor volume was calculated using the following formula: V = W2 × L/2 (W: the shortest diameter, L: the longest diameter). Then, the mice were sacrificed on day 17. The tumor node, lung, spleen and liver were removed and weighed and fixed in 10% buffered formalin for histological examination. All mouse experiments were performed with groups of five to six mice. The mice were randomly grouped into the treatment or corresponding control groups, and the operators were blinded to the group assignments.

Patient immune parameter analysis. Tumor specimens (n = 12) and peripheral blood (n = 13) were collected from 13 patients who underwent TIL-based ACT treatment at baseline and after CCRT and/or auto-TIL treatment. The peripheral immune subsets were detected by flow cytometry, the serum cytokine profile was measured using the cytokine Milliplex assay, and the tumor microenvironment biomarkers were analyzed by immunochemistry and immunofluorescence.

Serum cytokine profile analysis. Serum cytokine and chemokine levels in serum were measured using a cytokine Milliplex assay kit (Millipore Sigma) and MAGPIX Multiplexing System (Millipore Sigma) following the manufacturer's protocol.

Immunochemistry and immunofluorescence. Formalin-fixed paraffin-embedded tissue sections were continuously sectioned at a thickness of 4 μm, and an immunohistochemistry kit (Zhongshanjinqiao) was used according to the manufacturer's instructions. In brief, tissue sections were deparaffinized and

rehydrated by immersion in EDTA (pH 8.0) or 1x citrate (pH 6.0). A pressure cooker (95°C, 22 min) was applied for antigen retrieval. Goat serum was applied to block nonspecific binding sites at room temperature for 30 min. Primary antibodies, including anti-human PD-L1, anti-TOX, anti-Foxp3, and anti-CD56 antibodies, were incubated at 4°C overnight. The secondary antibody (Zhongshanjinqiao) was incubated for 30 min at room temperature. 3,3′-Diaminobenzidine tetrahydrochloride (DAB) was used for visualization. Finally, the pathological sections were counterstained with hematoxylin, dehydrated and sealed with neutral glue for optical microscopy.

For immunofluorescent staining of TILs, an Opal Polaris™ 7 color manual IHC kit (Akoya Biosciences) was used following the manufacturer's protocol with primary antibodies, including anti-human CD4, CD8 and CD20 antibodies. DAPI was used for nuclear staining and section mounting. Images were acquired using a PerkinElmer Vectra V.3.0 system, and Vectra software (Akoya Biosciences) and HALO software (Indica Labs) were used to analyze the images. Lymphocyte density was quantified as % of cells expressing a given marker of at least 5 high-power fields (HPFs). Mature TLSs correspond to lymphoid follicles, including a dense cellular aggregate resembling germinal centers found in secondary lymphoid structures (SLOs). The calculation of the immune combined score was as follows: 0 = low expression of PD-L1, TOX, or Foxp3 or high expression of CD4, CD8, CD20, CD56, or TLS; 1 = high expression of PD-L1, TOX, or Foxp3 or low expression of CD4, CD8, CD20, CD56, or TLS. The score was calculated by adding the expression of individual

markers. The maximum score was 8.

Statistics. The data analysis was mainly descriptive. Summary statistics for AEs, including the proportions of each preferred AE type were tabulated and assembled into Tables. AEs were categorized by grade. All correlative study results were treated as exploratory in nature due to the pilot status and sample size of the trial. Objective response will be plotted on applicable 'Waterfall' plots using percent change. For correlative analysis, we explored the extent to which changes between pre- and post-treatment levels correlate with response by t-test or Mann–Whitney U test. Furthermore, 2-tailed Student's t-tests, paired t-tests or Wilcoxon tests were performed for comparisons of 2 groups. A P value less than 0.05 was considered significant. All statistical analyses were performed using R software (version 4.0.3), GraphPad Prism 5 software (La Jolla, CA, USA) and SPSS 18.0 software (Chicago, IL, USA).

Study approval. This clinical trial was registered at https://register.clinicaltrials.gov (ClinicalTrials.gov NCT04443296). All patients provided written informed consent independently and agreed to donate specimens for scientific study. This study was approved by the Institutional Review Board of the Sun Yat-sen University Cancer Center (SYSUCC, B2019-124-01).

Data and materials availability. The study protocols are provided in the supplemental material. The key processed and clinical data have been deposited in the Research Data Deposit public platform (www.researchdata.org.cn) (accession code RDDA2022500226) to validate the authenticity of this study.

Author contributions

JL, HH and JHL conceived, designed and supervised the project. JL, HH and QL contributed to the implementation and design of the clinical study, writing of the protocol, statistical analysis and interpretation. XFL, BS, JHY and XZ contributed to the scRNA-sequence and bioinformation analysis. CPN, JXX, JH, and KL participated in the generation and expansion of TIL-infused product as well as laboratory testing. YLF, TW, MZ, YNZ, WJY, JDL, YFL, JYL, XPC, ZML and XSZ contributed to the recruitment and treatment of patients, data and trial management and review of the report. HH, JL, CPN, XZ and XFL were involved in the writing and revision of the manuscript. All authors have read and approved the manuscript. The order of co-first authors was determined by their efforts and contributions to the manuscript.

Competing interests

The authors have declared that no conflict of interest exists.

Acknowledgments

We thank all donors and patients for participating in the study. This work was supported by the National Key R&D Program (2018YFC1313400), Sci-Tech Key Program of the Guangzhou City Science Foundation (Grant No. 201802020001), and the Guangdong Province Sci-Tech International Key Program (Grant No. 2021A0505030027), and the National Natural Science Foundation of China (Grant Nos. 8197110786, 81773256, 81572982 and 82160557).

References

1. Cohen SS, et al. Obesity and screening for breast, cervical, and colorectal cancer in women: a review. *Cancer.* 2008;112(9):1892-904.
2. Gadducci A, and Cosio S. Neoadjuvant Chemotherapy in Locally Advanced Cervical Cancer: Review of the Literature and Perspectives of Clinical Research. *Anticancer research.* 2020;40(9):4819-28.
3. Chemoradiotherapy for Cervical Cancer Meta-Analysis C. Reducing uncertainties about the effects of chemoradiotherapy for cervical cancer: a systematic review and meta-analysis of individual patient data from 18 randomized trials. *J Clin Oncol.* 2008;26(35):5802-12.
4. Wright JD, et al. Prognostic Performance of the 2018 International Federation of Gynecology and Obstetrics Cervical Cancer Staging Guidelines. *Obstet Gynecol.* 2019;134(1):49-57.
5. Creelan BC, et al. Tumor-infiltrating lymphocyte treatment for anti-PD-1-resistant metastatic lung cancer: a phase 1 trial. *Nature medicine.* 2021;27(8):1410-8.
6. Dudley ME, et al. CD8+ enriched "young" tumor infiltrating lymphocytes can mediate regression of metastatic melanoma. *Clinical cancer research : an official journal of the American Association for Cancer Research.* 2010;16(24):6122-31.
7. Kradin RL, et al. Tumour-infiltrating lymphocytes and interleukin-2 in treatment of advanced cancer. *Lancet.* 1989;1(8638):577-80.
8. Weber J, et al. White paper on adoptive cell therapy for cancer with tumor-infiltrating lymphocytes: a report of the CTEP subcommittee on adoptive cell therapy. *Clinical cancer research : an official journal of the American Association for Cancer Research.* 2011;17(7):1664-73.
9. Stevanovic S, et al. A Phase II Study of Tumor-infiltrating Lymphocyte Therapy for Human Papillomavirus-associated Epithelial Cancers. *Clinical cancer research : an official journal of the American Association for Cancer Research.* 2019;25(5):1486-93.
10. Zsiros E, et al. Adoptive T-cell therapy is a promising salvage approach for advanced or recurrent metastatic cervical cancer. *J Clin Oncol.* 2015;33(14):1521-2.
11. Stevanovic S, et al. Complete regression of metastatic cervical cancer after treatment with human papillomavirus-targeted tumor-infiltrating T cells. *J Clin Oncol.* 2015;33(14):1543-50.
12. Tang B, et al. Safety and clinical activity with an anti-PD-1 antibody JS001 in advanced melanoma or urologic cancer patients. *J Hematol Oncol.* 2019;12(1):7.
13. van den Berg JH, et al. Tumor infiltrating lymphocytes (TIL) therapy in metastatic melanoma: boosting of neoantigen-specific T cell reactivity and long-term follow-up. *J Immunother Cancer.* 2020;8(2).
14. van der Kooij MK, et al. Phase I/II study protocol to assess safety and efficacy of adoptive cell therapy with anti-PD-1 plus low-dose pegylated-interferon-alpha in patients with metastatic melanoma refractory to standard of care treatments: the ACTME trial. *BMJ Open.* 2020;10(11):e044036.
15. Seitter SJ, et al. Impact of Prior Treatment on the Efficacy of Adoptive Transfer of Tumor-Infiltrating Lymphocytes in Patients with Metastatic Melanoma. *Clinical cancer research : an official journal of the American Association for Cancer Research.* 2021.
16. Khammari A, et al. Adoptive TIL transfer in the adjuvant setting for melanoma: long-term patient survival. *J Immunol Res.* 2014;2014(186212.

17. Li J, et al. Phase I trial of adoptively transferred tumor-infiltrating lymphocyte immunotherapy following concurrent chemoradiotherapy in patients with locoregionally advanced nasopharyngeal carcinoma. *Oncoimmunology.* 2015;4(2):e976507.
18. Sorbe B, et al. Combined external and intracavitary irradiation in treatment of advanced cervical carcinomas: predictive factors for local tumor control and early recurrences. *Int J Oncol.* 2010;36(2):371-8.
19. Morris M, et al. Pelvic radiation with concurrent chemotherapy compared with pelvic and para-aortic radiation for high-risk cervical cancer. *N Engl J Med.* 1999;340(15):1137-43.
20. Eifel PJ, et al. Pelvic irradiation with concurrent chemotherapy versus pelvic and para-aortic irradiation for high-risk cervical cancer: an update of radiation therapy oncology group trial (RTOG) 90-01. *Journal of clinical oncology : official journal of the American Society of Clinical Oncology.* 2004;22(5):872-80.
21. Rose PG, et al. Concurrent cisplatin-based radiotherapy and chemotherapy for locally advanced cervical cancer. *N Engl J Med.* 1999;340(15):1144-53.
22. Rose PG, et al. Outcome of stage IVA cervical cancer patients with disease limited to the pelvis in the era of chemoradiation: a Gynecologic Oncology Group study. *Gynecol Oncol.* 2011;121(3):542-5.
23. Colombo N, et al. Pembrolizumab for Persistent, Recurrent, or Metastatic Cervical Cancer. *The New England journal of medicine.* 2021;385(20):1856-67.
24. Romero D. Pembrolizumab tunes up chemotherapy in cervical cancer. *Nature reviews Clinical oncology.* 2021;18(12):747.
25. Besser MJ, et al. Adoptive cell therapy for metastatic melanoma patients: pre-clinical development at the Sheba Medical Center. *Isr Med Assoc J.* 2006;8(3):164-8.
26. Besser MJ, et al. Clinical responses in a phase II study using adoptive transfer of short-term cultured tumor infiltration lymphocytes in metastatic melanoma patients. *Clinical cancer research : an official journal of the American Association for Cancer Research.* 2010;16(9):2646-55.
27. Besser MJ, et al. Adoptive transfer of tumor-infiltrating lymphocytes in patients with metastatic melanoma: intent-to-treat analysis and efficacy after failure to prior immunotherapies. *Clinical cancer research : an official journal of the American Association for Cancer Research.* 2013;19(17):4792-800.
28. Khammari A, et al. Long-term follow-up of patients treated by adoptive transfer of melanoma tumor-infiltrating lymphocytes as adjuvant therapy for stage III melanoma. *Cancer immunology, immunotherapy : CII.* 2007;56(11):1853-60.
29. Dreno B, et al. Randomized trial of adoptive transfer of melanoma tumor-infiltrating lymphocytes as adjuvant therapy for stage III melanoma. *Cancer immunology, immunotherapy : CII.* 2002;51(10):539-46.
30. Nam EJ, et al. Comparison of carboplatin- and cisplatin-based concurrent chemoradiotherapy in locally advanced cervical cancer patients with morbidity risks. *Oncologist.* 2013;18(7):843-9.
31. Sebastiao AM, et al. Carboplatin-based chemoradiotherapy in advanced cervical cancer: an alternative to cisplatin-based regimen? *Eur J Obstet Gynecol Reprod Biol.* 2016;201(161-5.
32. Andersen R, et al. Long-Lasting Complete Responses in Patients with Metastatic Melanoma after Adoptive Cell Therapy with Tumor-Infiltrating Lymphocytes and an Attenuated IL2

Regimen. *Clinical cancer research : an official journal of the American Association for Cancer Research.* 2016;22(15):3734-45.
33. Yang JC. Toxicities Associated With Adoptive T-Cell Transfer for Cancer. *Cancer J.* 2015;21(6):506-9.
34. Huang H, et al. Effectiveness of Sequential Chemoradiation vs Concurrent Chemoradiation or Radiation Alone in Adjuvant Treatment After Hysterectomy for Cervical Cancer: The STARS Phase 3 Randomized Clinical Trial. *JAMA Oncol.* 2021;7(3):361-9.
35. Dudley ME, et al. Adoptive cell transfer therapy following non-myeloablative but lymphodepleting chemotherapy for the treatment of patients with refractory metastatic melanoma. *J Clin Oncol.* 2005;23(10):2346-57.
36. Bockel S, et al. [Immunotherapy and radiotherapy]. *Cancer Radiother.* 2017;21(3):244-55.
37. Hallahan D, et al. Cell adhesion molecules mediate radiation-induced leukocyte adhesion to the vascular endothelium. *Cancer research.* 1996;56(22):5150-5.
38. McGinnes K, et al. The effect of radiotherapy on the natural killer (NK)-cell activity of cancer patients. *J Clin Immunol.* 1987;7(3):210-7.
39. Bos PD, et al. Transient regulatory T cell ablation deters oncogene-driven breast cancer and enhances radiotherapy. *The Journal of experimental medicine.* 2013;210(11):2435-66.
40. Goff SL, et al. Randomized, Prospective Evaluation Comparing Intensity of Lymphodepletion Before Adoptive Transfer of Tumor-Infiltrating Lymphocytes for Patients With Metastatic Melanoma. *J Clin Oncol.* 2016;34(20):2389-97.
41. Rothermel LD, et al. Identification of an Immunogenic Subset of Metastatic Uveal Melanoma. *Clinical cancer research : an official journal of the American Association for Cancer Research.* 2016;22(9):2237-49.
42. Butterfield LH, et al. Generation of melanoma-specific cytotoxic T lymphocytes by dendritic cells transduced with a MART-1 adenovirus. *Journal of immunology.* 1998;161(10):5607-13.
43. Wang YL, et al. Lymphocytes infiltrating human ovarian tumors: synergy between tumor necrosis factor alpha and interleukin 2 in the generation of CD8+ effectors from tumor-infiltrating lymphocytes. *Cancer research.* 1989;49(21):5979-85.
44. Dudley ME, et al. Adoptive cell therapy for patients with metastatic melanoma: evaluation of intensive myeloablative chemoradiation preparative regimens. *J Clin Oncol.* 2008;26(32):5233-9.
45. Lheureux S, et al. Association of Ipilimumab With Safety and Antitumor Activity in Women With Metastatic or Recurrent Human Papillomavirus-Related Cervical Carcinoma. *JAMA Oncol.* 2018;4(7):e173776.
46. Cariani E, et al. Immunological and molecular correlates of disease recurrence after liver resection for hepatocellular carcinoma. *PLoS One.* 2012;7(3):e32493.
47. Hashemi S, et al. Surprising impact of stromal TIL's on immunotherapy efficacy in a real-world lung cancer study. *Lung Cancer.* 2021;153(81-9.
48. Katz SC, et al. T cell infiltrate and outcome following resection of intermediate-grade primary neuroendocrine tumours and liver metastases. *HPB (Oxford).* 2010;12(10):674-83.
49. Schwartzentruber DJ, et al. In vitro predictors of therapeutic response in melanoma patients receiving tumor-infiltrating lymphocytes and interleukin-2. *J Clin Oncol.* 1994;12(7):1475-83.
50. Takada K, et al. Prediction of distant metastatic recurrence by tumor-infiltrating lymphocytes in hormone receptor-positive breast cancer. *BMC Womens Health.* 2021;21(1):225.

51. Willsmore ZN, et al. B Cells in Patients With Melanoma: Implications for Treatment With Checkpoint Inhibitor Antibodies. *Frontiers in immunology.* 2020;11(622442.
52. Liu C, et al. A portable and cost-effective microfluidic system for massively parallel single-cell transcriptome profiling. *bioRxiv.* 2019.
53. McGinnis CS, et al. DoubletFinder: Doublet Detection in Single-Cell RNA Sequencing Data Using Artificial Nearest Neighbors. *Cell systems.* 2019;8(4):329-37.e4.
54. Stuart T, et al. Comprehensive Integration of Single-Cell Data. *Cell.* 2019;177(7):1888-902 e21.
55. Wickham H. *ggplot2: Elegant Graphics for Data Analysis.* Springer-Verlag New York; 2016.
56. Wu T, et al. clusterProfiler 4.0: A universal enrichment tool for interpreting omics data. *Innovation.* 2021;2(3):100141.
57. Caushi JX, et al. Transcriptional programs of neoantigen-specific TIL in anti-PD-1-treated lung cancers. *Nature.* 2021;596(7870):126-32.
58. Li H, et al. Dysfunctional CD8 T Cells Form a Proliferative, Dynamically Regulated Compartment within Human Melanoma. *Cell.* 2019;176(4):775-89 e18.
59. Whitfield ML, et al. Common markers of proliferation. *Nature reviews Cancer.* 2006;6(2):99-106.

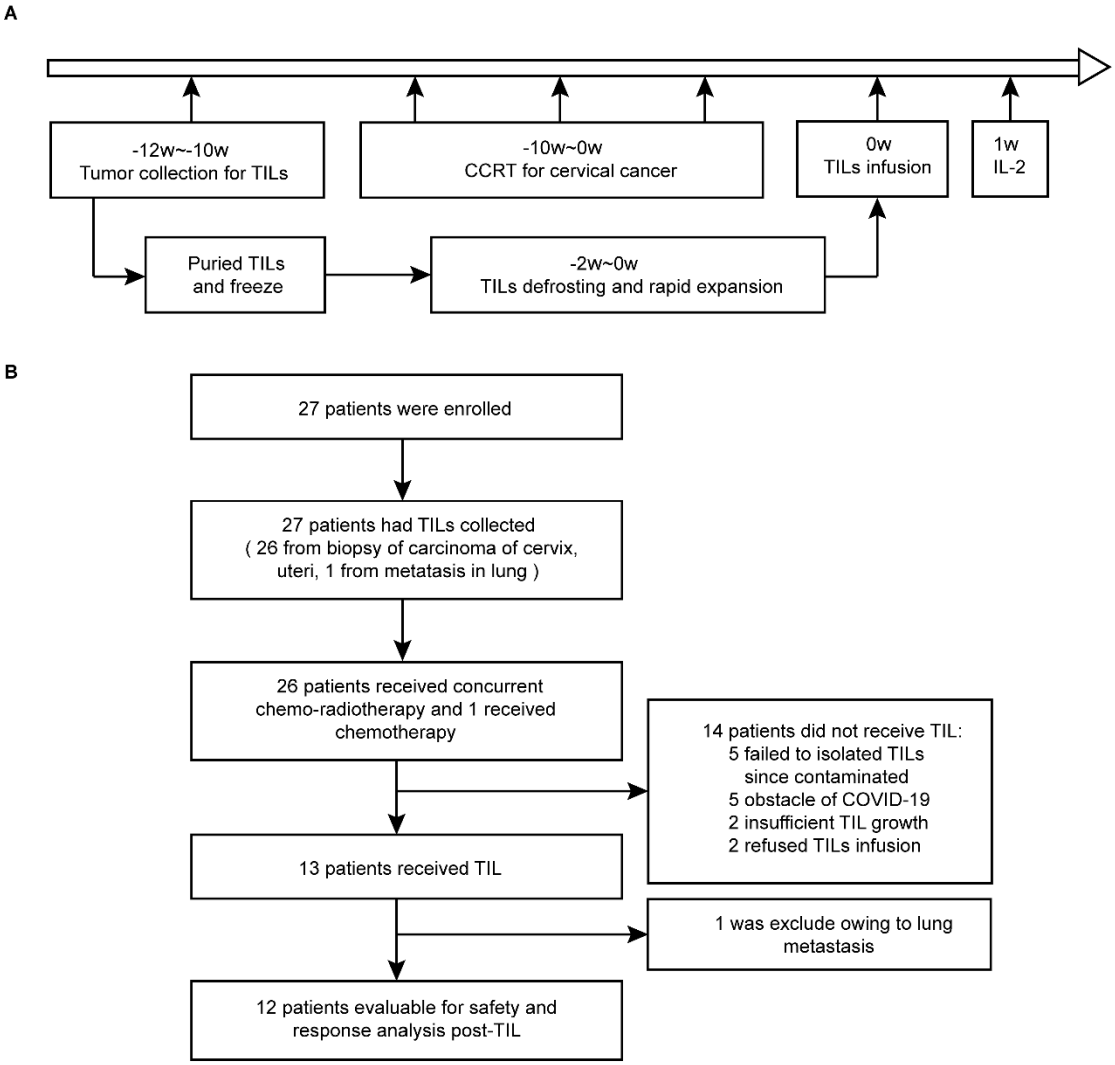

Figure 1. Schematic representing the study design and patient disposition. (**A**) Clinical trial schema. The week count is relative to TIL infusion. (**B**) Patient flow chart. Of the 27 patients enrolled, 13 patients received TIL infusion after CCRT (12 patients) or chemotherapy (1 patient) and were evaluated for safety and tumor response. CCRT, concurrent chemoradiotherapy, radical radiotherapy for cervical cancer with concurrent cisplatin 30~40 mg/m^2 weekly during external radiotherapy; CT, chemotherapy.

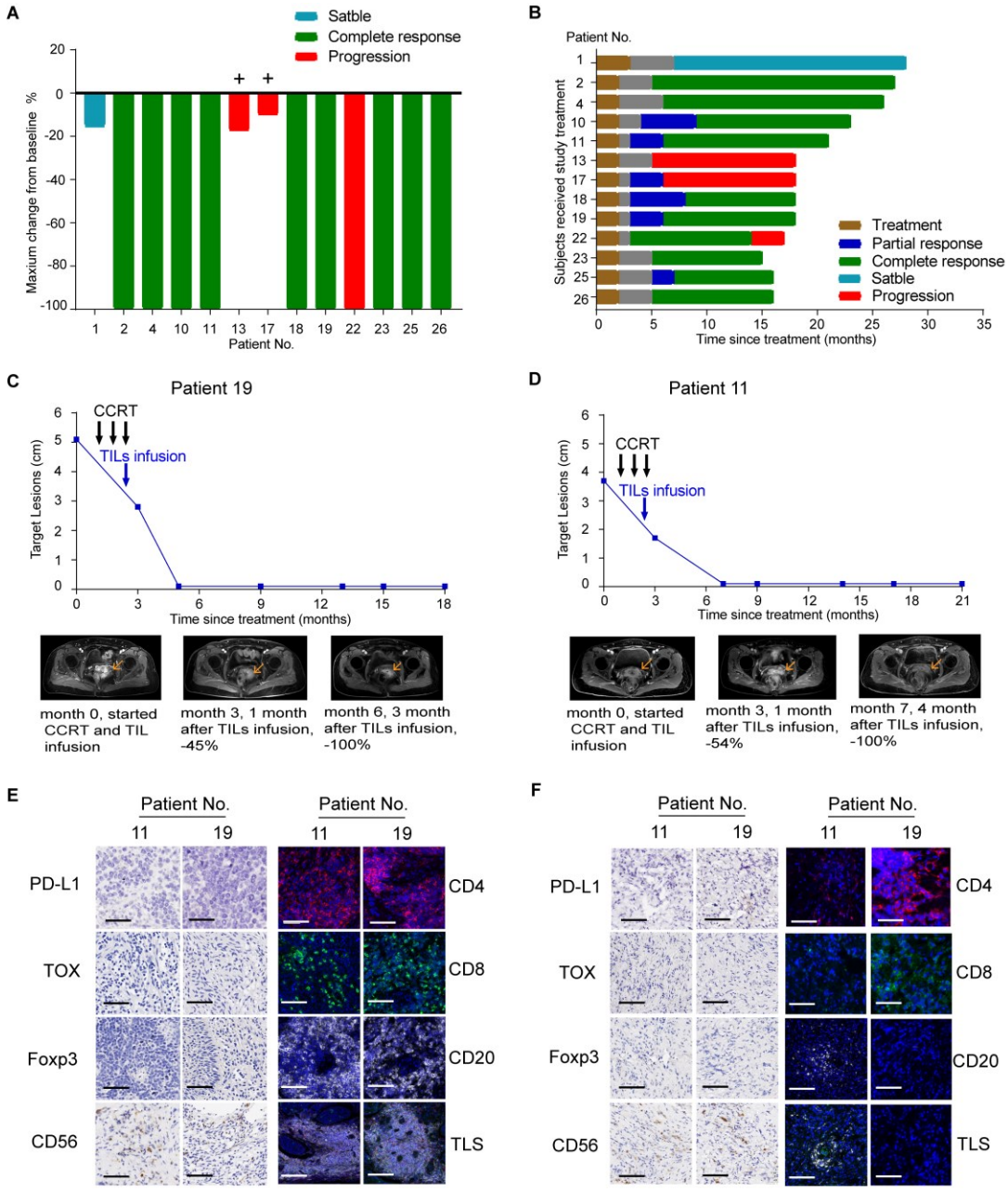

Figure 2. Patient clinical and immune evaluation for CCRT and auto-TIL treatment. (A) Waterfall plot of the maximum change in the sum of target lesion (primary tumor lesion of the uterine cervix) compared with baseline measurements in 13 patients. CR, complete response; PR, partial response; PD, progressive disease; SD, stable disease; +, distant metastasis. Patient No. 13, 17 presented with distant lung and bone metastasis. Patient No. 22 had pelvic recurrence after a 9-month CR. **(B)**

Swimmer plots of the change in the sum of target lesions from the treatment in 13 patients. Each bar represents one subject in this study. **(C-D)** MRI scans obtained at baseline and after CCRT and TIL infusion for Patient Nos. 11 and 19 with cervical cancer. **(E-F)** Representative IHC and IF images of Patient Nos. 11 and 19 showing PD-L1, TOX, Foxp3, CD56, CD4 (red), CD8 (green), and CD20 (white) expression and multiplex immunofluorescence staining showing TLSs composed of $CD20^+$, $CD4^+$ and $CD8^+$ cells at baseline (E) and after CCRT treatment (F). The scale bar denotes 50 μm or 100 μm for IHC or IF, respectively, and DAPI (blue) is used for nuclear staining. Original magnification ×10.

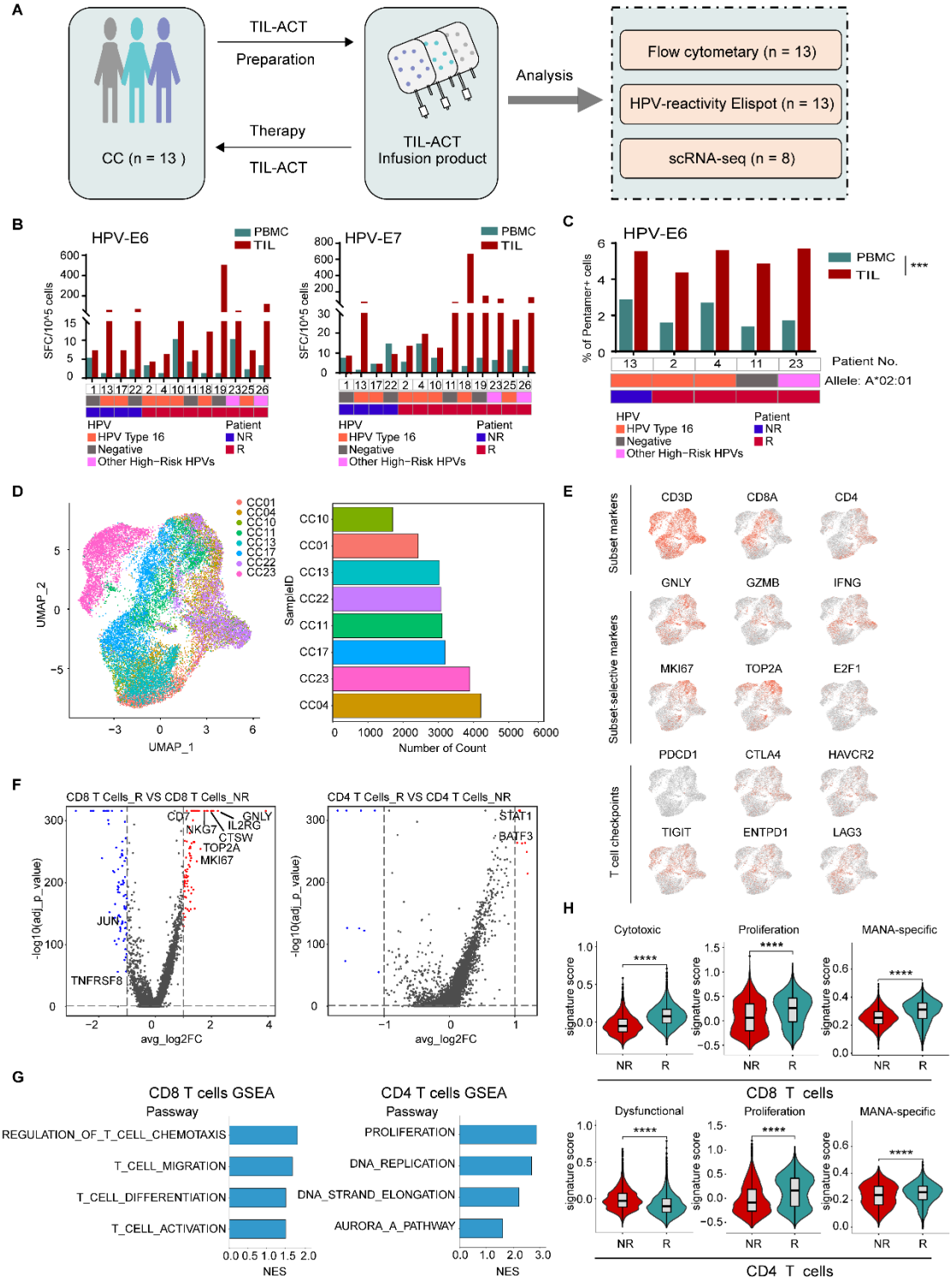

Figure 3. Correlations of characteristics of infused TIL products and clinical response. (A) Schematic illustration of biomarkers and functional identification of TIL products in this study. **(B)** The frequency of reactivity T cells against HPV E6 (left) and E7 (right) antigens in peripheral blood and TILs (n = 13). **(C)** The frequency

of HPV E6 antigen-specific T cells in peripheral blood and TILs from HLA-A2-positive CC patients (n = 5). **(D)** UMAP plot showing cells from 8 CC patients and the bar graph showing the number of cells from the corresponding patient origin (n = 8). **(E)** Expression and distribution of canonical T cell marker genes (CD3D, CD8A and CD4) and genes related to cytotoxicity and proliferation among these cell subsets. **(F)** Volcano plots showing DEGs in CD8 T cells (left) and CD4 T cells (right) in responders vs. nonresponders. Representative genes are labeled. **(G)** GSEA shows the pathway activities in CD8 T cells (left) and CD4 T cells (right) between responders and nonresponders. **(H)** Violin plots show the key signature scores of CD8 T cells (top) and CD4 T cells (bottom) (responders vs. nonresponders). MANA, mutation-associated neoantigens. *P < 0.05, ****P < 0.0001, Mann–Whitney test or Wilcox test.

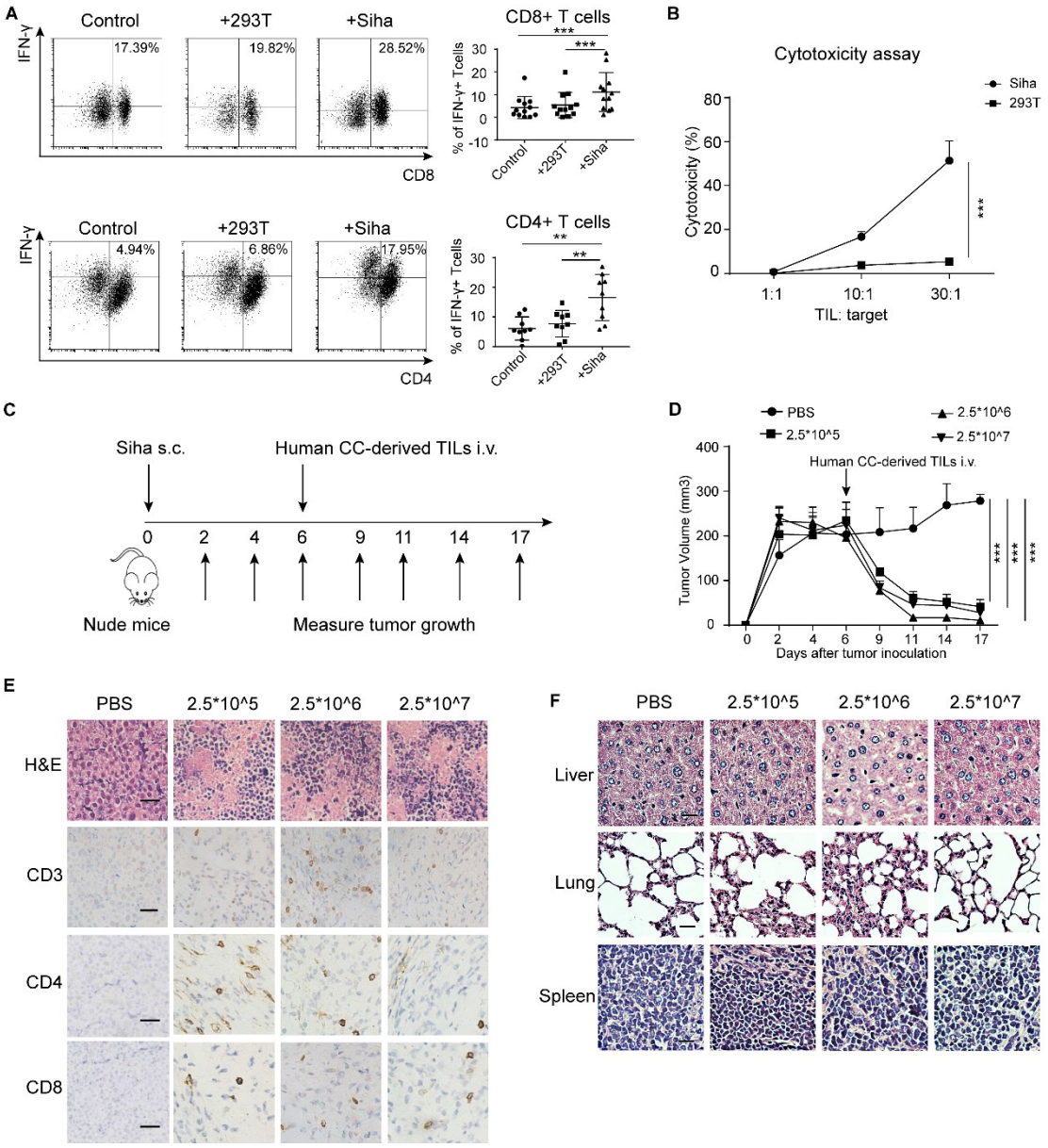

Figure 4. Specific cytotoxic effects and antitumor effects of TILs in vitro and in vivo. (A) Representative flow cytometry plots (left) and summary graphs (right) showing the frequencies of IFN-γ-producing T cells among $CD4^+$ (n = 9) and $CD8^+$ (n = 12) TILs cocultured with Siha and 293T cells. **(B)** LDH cytotoxicity assay showing the specific killing effect of TILs (n = 3). **(C)** Experimental scheme for monitoring tumor growth and TIL therapy. **(D)** Time course of tumor growth in different groups adoptively transferred with human TILs isolated from CC patients or not. n = 5, the data are shown as the mean ± s.e.m. ***P ≤ 0.001, Mann–Whitney test. **(E)**

Representative images of HE staining of transplanted tumors and representative images of IHC of anti-human CD3, CD4 and CD8 in the tumor microenvironment. **(F)** Representative images of HE staining of the liver, lung, and spleen of nude mice in each experimental group. Scale bar, 100 μm.

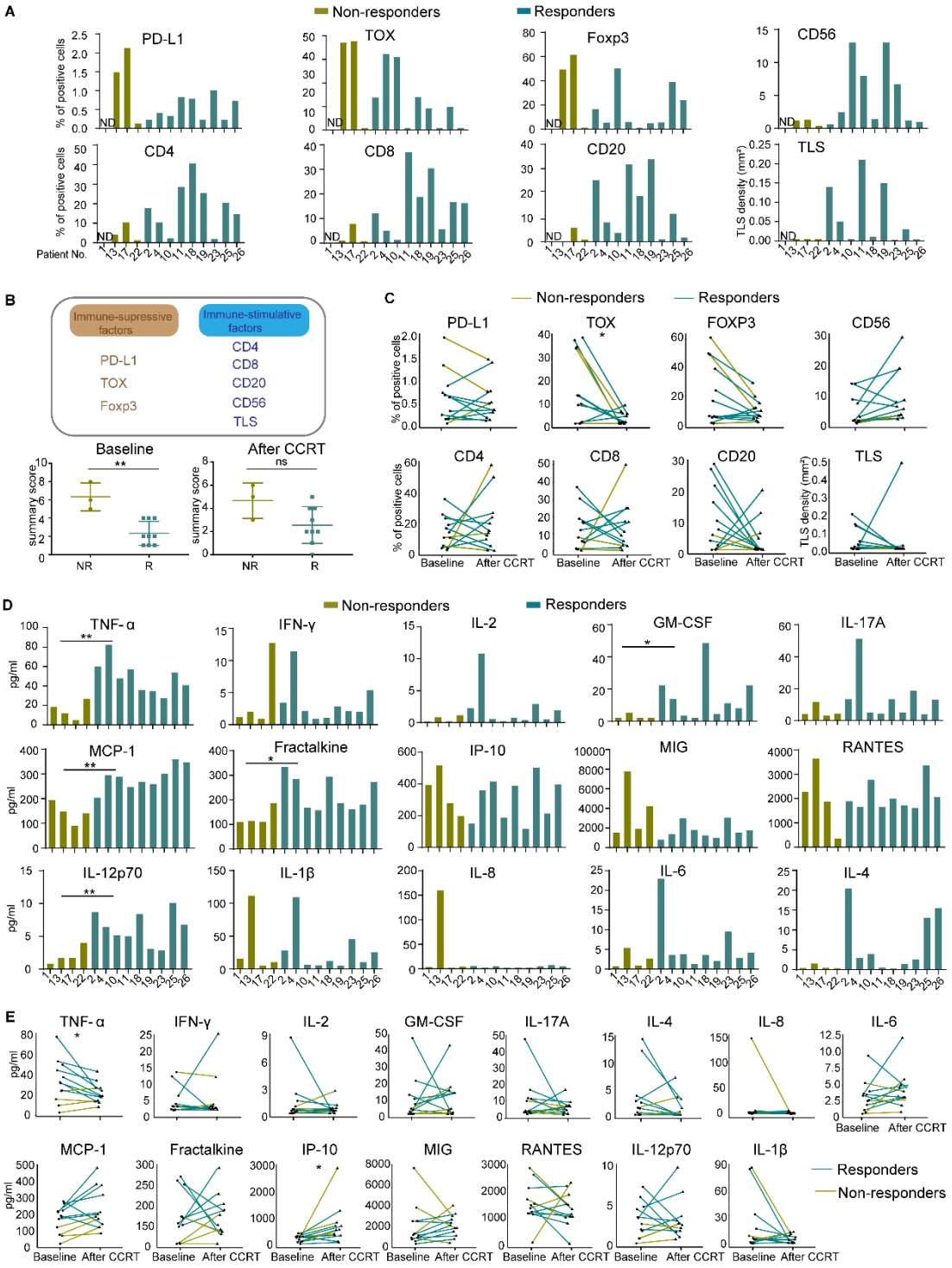

Figure 5. Linkage of baseline biomarkers and dynamic changes in biomarkers

after CCRT to clinical response. (A) The levels or numbers of indicative biomarkers, including PD-L1, TOX, Foxp3, CD4, CD8, CD56, CD20 and TLS, in 12 tumor specimens from CC patients at baseline (9 responders and 3 nonresponders). **(B)** Immune factors (top) in the tumor microenvironment (TME) were divided into immune-suppressive factors (PD-L1, TOX, Foxp3) and immune-stimulative factors (CD4, CD8, CD20, CD56, TLS) according to the function of the gene or the indicated cell population (bottom). The combined immune score of PD-L1, TOX, Foxp3, CD4, CD8, CD20, CD56, and TLS at baseline (left) and after CCRT (right) in responders (R, n = 9) vs. nonresponders (NR, n = 3). The calculation of the combined immune score is described in the Supplemental Method section. **(C)** Changes in indicative biomarkers in CC specimens before and after CCRT (n = 12). **(D)** Histogram showing the levels of serum cytokine and chemokine levels, including TNF-a, fractalkine, IL-12p70, MCP-1, IFN-γ, IL-2, IL-1b, IL-17a, IL-4, IL-6, GM-CSF, RANTES, IP-10, IL-8 and MIG, at baseline in responders (R, n = 9) and nonresponders (NR, n = 4). **(E)** Changes in indicative serum cytokines and chemokines in CC patients at baseline vs. after CCRT (n = 13). *P < 0.05, Mann–Whitney test for nonparametric data. A paired t test was used to determine significance for all comparisons at baseline and after CCRT

Table 1 Characteristics and clinical responses of recruited patients

Patients who received CCRT + TIL infusion + intramuscular IL-2 injections

Patient No.	Age	Histology	Disease site	Stage	HPV type	Treatment	Infused TIL number (*10^9)	Response (duration in months)	PFS (months)	OS (months)
1	64	AC	Cervix, lung	IVB	Negative	CTx3 TIL infusion	3.35	SD (21)	7	28
2	61	SSC	Cervix	IIIB	Type 16	CTx3, RT TIL infusion	2.33	CR (22)	27	27
4	52	SSC	Cervix	IIIB	Type 16	CTx3, RT TIL infusion	2.8	CR (19)	26	26
10	54	SSC	Cervix, uterus, urinary system, lymph nodes	IIIC1r	Type 16	CTx3, RT TIL infusion	3.9	CR (14)	23	23
11	64	SSC	Cervix, uterus, vaginal vault	IIIB	Negative	CTx3, RT TIL infusion	2.85	CR (15)	21	21
13	53	SSC	Cervix, lymph nodes	IIIB	Type 16	CTx3, RT TIL infusion	4.3	PD (13)	5	18
17	56	SSC	Cervix, vagina, uterus, para-uterus	IIIB	Type 16	CTx3, RT TIL infusion	3.38	PD (12)	6	18
18	46	SSC	Cervix, lymph nodes	IIIC	Type 16	CTx3, RT TIL infusion	1.2	CR (10)	18	18
19	56	SSC	Cervix, vagina, para-uterus	IIIB	Negative	CTx2, RT TIL infusion	1.5	CR (12)	18	18
22	65	SSC	Cervix, para-uterus	IIIB	Negative	CTx3, RT TIL infusion	3.24	PD (3)	14	17
23	71	SSC	Cervix, lymph nodes	IIIB	Other High-risk HPVs	CTx3, RT TIL infusion	1.21	CR (10)	15	15
25	57	AC	Cervix, lymph nodes	IIIB	Type 16	CTx2, RT TIL infusion	1.37	CR (9)	14	14
26	56	SSC	Cervix, lymph nodes	IIIC1r	Other High-risk HPVs	CTx2, RT TIL infusion	3.42	CR (11)	14	14
Patients who received CCRT only										
3	55	SSC	Cervix	IIIB	Other High-risk HPVs	CTx5, RT Insufficient TIL growth*	-	CR (18)	26	26
5	62	SSC	Cervix, lymph nodes	IIIC1r	NA	CTx3, RT	-	Death	6	22

						Failed to isolate TILs due to contamination*				
6	58	SSC	Cervix, para-uterus	IIIB	Type 16	CTx1, RT Failed to isolate TILs due to contamination*	-	CR (19)	25	25
7	49	AC	Cervix, para-uterus	IIIA	Type 16	Refused treatment	-	NA	NA	NA
8	65	SSC	Cervix, lymph nodes	IIIC1r	Type 16	CTx2, RT Hindered by the influence of COVID-19*	-	CR (19)	25	25
9	54	SSC	Cervix, lymph nodes	IIIC1r	Type 16	CTx2, RT Refused TIL infusion*	-	CR (17)	23	23
12	62	SSC	Cervix, vagina	IIIB	Type 16	CTx2, RT Hindered by the influence of COVID-19*	-	CR (15)	20	20
14	42	SSC	Cervix, vagina, para-uterus	IIIB	Negative	CTx2, RT Hindered by the influence of COVID-19*	-	CR (12)	20	20
15	65	SSC	Cervix, vagina, para-uterus, lymph nodes	IIIC2r	Type 16	CTx3, RT Hindered by the influence of COVID-19*	-	Death	9	17
16	51	SSC	Cervix, vagina, lymph nodes	IIIB	Negative	CTx2, RT Hindered by the influence of COVID-19*	-	PR (10)	18	18
20	54	SSC	Cervix, vagina, para-uterus, lymph nodes	IIIB	Negative	CTx2, RT Failed to isolate TILs due to contamination*	-	CR (12)	18	18
21	57	SSC	Cervix, vagina, para-uterus	IVA	Negative	CTx2, RT Failed to isolated TILs due to contamination*	-	CR (12)	17	17
24	65	SSC	Cervix, vagina, para-uterus	IIIB	Negative	CTx2, RT Failed to isolated TILs due to contamination*	-	PR (6)	15	15
27	52	SSC	Cervix, lymph nodes	IIIC2r	Negative	CTx2, RT Insufficient TIL growth*	-	CR (9)	14	14

Abbreviations: AC, adenocarcinoma; SCC, squamous cell carcinoma; CR, complete response; PD, progressive disease; PR, partial response; SD, stable disease; CCRT, concurrent chemoradiotherapy; CT, chemotherapy; PFS, progression-free survival; OS, overall survival; NA, not available; * Reason for failure of TIL infusion.

Table 2. Adverse events of all recruited patients with or without auto-TIL infusion following CCRT

Adverse events	Patients who received CCRT and TIL infusion and intramuscular IL-2 injections (n=12)					Patients who received CCRT only (n = 14)		
	CCRT-related		ACT- and IL-2-related		Any	CCRT-related		Any
	Grade 1/2 n (%)	Grade 3/4 n (%)	Grade 1/2 n (%)	Grade 3/4 n (%)	n (%)	Grade 1/2 n (%)	Grade 3/4 n (%)	n (%)
Leukopenia	6 (50.0)	1 (8.3)	0	0	7 (58.3)	9 (64.3)	2 (14.3)	11 (78.6)
Neutropenia	2 (16.7)	1 (8.3)	0	0	3 (25.0)	3 (21.4)	3 (21.4)	6 (42.9)
Anemia [c]	5 (41.7)	4 (33.3)	0	0	9 (75.0)	7 (50.0)	3 (21.4)	10 (71.4)
Thrombocytopenia	1 (8.3)	3 (25.0)	0	0	4 (33.3)	2 (14.3)	1 (7.1)	3 (21.4)
Transaminase abnormality	1 (8.3)	0	0	0	1 (8.3)	1 (7.1)	0	1 (7.1)
Hypokalemia	5 (41.7)	0	0	0	5 (41.7)	3 (21.4)	0	3 (21.4)
Creatinine increased	1 (8.3)	0	0	0	1 (8.3)	1 (7.1)	0	1 (7.1)
Hypoalbuminemia	1 (8.3)	0	0	0	1 (8.3)	0	0	0
Nausea	6 (50.0)	0	0	0	6 (50.0)	9 (64.3)	0	9 (64.3)
Vomiting	2 (16.7)	0	0	0	2 (16.7)	4 (28.6)	0	4 (28.6)
Diarrhea	6 (50.0)	0	0	0	6 (50.0)	6 (42.9)	0	6 (42.9)
Abdominal pain	2 (16.7)	0	0	0	2 (16.7)	4 (28.6)	0	4 (28.6)
Constipation	3 (25.0)	0	0	0	3 (25.0)	1 (7.1)	0	1 (7.1)
Allergy	0	0	1 (8.3)	1 (8.3)	2 (16.7)	0	0	0
Fatigue	4 (33.3)	0	1 (8.3)	0	5 (41.7)	2 (14.3)	0	2 (14.3)
Fever	1 (8.3)	0	7 (58.3)	0	8 (66.7)	0	0	0